Electronic Materials Letters, Vol. 2, No. 2 (2006), pp. 119-126

Synthesis and Electrochemical Performances of $LiNi_{0.4}Mn_{0.4}Co_{0.2}O_2$ Cathode Material for Lithium Rechargeable Battery

Hyun-Soo Kim[1,*], Ke-Tack Kim[1], and Padikkasu Periasamy[2]

[1]Korea Electrotechnology Research Institute, Changwon 641-120, South Korea
[2]Central Electrochemical Research Institute, Tamil Nadu 630 006, INDIA

Layered $LiNi_{0.4}Mn_{0.4}Co_{0.2}O_2$ powder was synthesized via a solution combustion method using a glycine. The effects of temperature in the heat treatment on the powder and its performance were studied. X-ray diffraction patterns indicated that pure single-phase $LiNi_{0.4}Mn_{0.4}Co_{0.2}O_2$ was obtained. Charge-discharge behaviors indicated that a sample prepared at 750 °C for 24 hrs showed a best specific discharge capacity of 159.5 $mAhg^{-1}$ after the 20th cycle in the voltage between 3.0 and 4.6 V. Electrochemical impedance studies showed a decrease in charge transfer resistance at the high state of charge.

Keywords: combustion process, glycine fuel, $LiNi_{0.4}Mn_{0.4}Co_{0.2}O_2$ materials, charge transfer resistance, state of charge

1. INTRODUCTION

Lithium-ion batteries have been widely used as power sources for modern portable electronic devices, such as laptop computers, cellular phones, and camcorders. Among available rechargeable batteries, lithium-ion batteries have the highest energy density and the longest cycle life. Large-scale lithium-ion batteries also have a great potential for electric vehicles and stationary energy storage systems, and they are dominating the rechargeable battery market, replacing alkaline nickel-cadmium and nickel-metal hydride batteries due to their excellent performance. The electrochemical properties of cathode materials in lithium-ion batteries are very critical for the overall battery performance. The operation of lithium-ion batteries relies on the extraction and insertion of lithium ions in both cathode and anode hosts.

The lithium-ion source, however, is provided entirely by cathode materials. A number of studies on lithium transition metal oxides have been performed relating to electrode materials for lithium batteries. Such studies have led to the development of layered $LiCoO_2$, $LiNiO_2$, and spinel $LiMn_2O_4$ as cathode materials for lithium-ion batteries[1-3]. Among these layered oxides, the structurally ordered $LiNiO_2$ compound is difficult to synthesize. In addition, its multi-phase reaction occurs during electrochemical cycling leads to structural degradation and poor cycleability[4]. Similarly, $LiMn_2O_4$ spinels have serious problems, such as Mn dissolution and large capacity loss at elevated temperatures[5]. To date, $LiCoO_2$ cathode materials have been widely used in commercial lithium-ion batteries. However, $LiCoO_2$ compounds are expensive, toxic, and environmentally harmful. Furthermore, the specific capacity of $LiCoO_2$ is limited to about 145 $mAhg^{-1}$. Therefore, it is necessary to develop new cathode compounds for lithium-ion batteries that are cost-effective and non-toxic, while having good electrochemical performance.

Hence, iso-structural solid solutions of the general formula $LiNi_{1-y}Co_yO_2$ have been studied for their electrochemical properties[6, 7]. Recently, the concept of a one-to-one, solid-state mixture of $LiNiO_2$ and $LiMnO_2$, i.e., $LiNi_{0.5}Mn_{0.5}O_2$, was introduced by Makimura and Ohzuku[8], and the electrochemical cycling behavior of $LiNi_{0.5}Mn_{0.5}O_2$ was proven to be superior to the end members. Subsequently, Lu *et al.* reported that $LiNi_{0.5}Mn_{0.5}O_2$, having the same crystallographic structure as $LiCoO_2$, $LiNiO_2$, and $LiNi_{0.8}Co_{0.2}O_2$, exhibits excellent cycleability, with a stable specific discharge capacity of 150 $mAhg^{-1}$ between 2.5 and 4.3 V and a specific discharge capacity of 160 $mAhg^{-1}$ between 2.0 and 4.6 V[9]. In T2-$Li_{2/3}[Ni_{1/3}Mn_{2/3}]O_2$, the Ni and Mn atoms are believed to be in the +2 and +4 oxidation state when Li is extracted electrochemically from $Li_{2/3}[Ni_{1/3}Mn_{2/3}]O_2$[10]. Lu *et al.*[11] studied the electrochemical behaviors of $Li[Ni_xCo_{1-2x}Mn_x]O_2$ compounds, and they proposed that the empirical formula for layered $Li[Ni_xCo_{1-2x}Mn_x]O_2$ compounds should satisfy two rules, as follows. First, the sum of the cation occupation on the 3b sites of space group R3m in the transition metal layers must equal one. Second, the sum of the cat-

*Corresponding author: hskim@keri.re.kr

ion oxidation state must equal three. Based on these rules, they synthesized $Li[Ni_xCo_{1-2x}Mn_x]O_2$ (x=1/4 and 3/8) by the "mixed hydroxide" method, and these compounds showed good electrochemical properties.

The mixed hydroxide method, however, is more complicated than conventional solid-state reaction methods. Therefore, in this paper, we report on $LiNi_{0.4}Mn_{0.4}Co_{0.2}O_2$ compounds that were prepared using a glycine-assisted combustion solution method. Both the preparation method and the electrochemical properties of the developed compounds were discussed.

2. EXPERIMENTAL

Crystalline powders of $LiNi_{0.4}Mn_{0.4}Co_{0.2}O_2$ were synthesized via a combustion method. Stoichiometric amounts of aqueous solutions of nitrates of lithium, nickel, manganese, and cobalt (Aldrich) were thoroughly ground in an agate mortar, dissolved in distilled water, and mixed with an aqueous solution of glycine. The glycine acted as a fuel for the spontaneous combustion of the mixed solution at elevated temperatures. The precursor solution was heated at 100 °C for 1 hr to obtain a viscous solution. The viscous solution was dried at 120 °C for 12 hrs; then, it was further heated to 300 °C and 600 °C for 3 hrs, and 750 °C for 3, 12, and 24 hrs.

Thermal decomposition behavior of the precursor $LiNi_{0.4}Mn_{0.4}Co_{0.2}O_2$ was examined by thermo gravimetric analysis (TGA) in air using a Perkin Elmer TGA7 analyzer at a heating rate of 10 min^{-1}. The typical weight of the sample was around 5 mg. The phase purity of the products was verified using a Philips X-ray diffractometer. The diffractograms were recorded using nickel-filtered Cukα radiation at room temperature in the 2θ range of 10 - 80 ° with a scan rate of 0.02 $^{o}s^{-1}$.

Cyclic voltammetric studies were carried out using lithium metal foil to serve as the counter and reference electrodes, with $LiNi_{0.4}Mn_{0.4}Co_{0.2}O_2$ as the working electrode. Cyclic voltammograms were run on an IM6 electrochemical instrument at a scan rate of 100 $Vsec^{-1}$ between 3.0 to 4.8 V, and 1 M solution of $LiPF_6$ in EC/DEC (1:1) was used as electrolyte. The impedance spectra were recorded with 2016 coin cells on an IM6 electrochemical instrument setup between 1 MHz and 1 kHz. The cells were galvanostatically charged to various states of charge prior to recording the impedances plots.

Positive electrodes were prepared using a slurry of 85 % active material, 5 % super-P carbon, and 10 % PVdF binder in NMP (N-methyl-2-pyrrolidone). The slurry was coated on an aluminum foil and dried at 110 °C for 3 - 4 hrs in an oven. Then, the dried electrode was roll-pressed and punched out using a punching machine. The thickness of the electrodes was around 60 - 70 μm. The electrochemical cells were assembled in standard 2016 coin cell hardware. A lithium metal foil and $LiNi_{0.4}Mn_{0.4}Co_{0.2}O_2$ were used for both the anode and the cathode. Initially, the cells were cycled at a 0.1C rate between 3.0 and 4.6 V in a multi-channel battery life cycle tester (MACCOR 4000) to evaluate the performance of the $LiNi_{0.4}Mn_{0.4}Co_{0.2}O_2$ powders.

3. RESULTS AND DISCUSSION

The thermogram pattern of the dried precursor sample of $LiNi_{0.4}Mn_{0.4}Co_{0.2}O_2$ heated from 30 to 800 °C is shown in Fig. 1. The precursor curves exhibit three steps with weight loss. The first step, which was observed between 30 and 100 °C , showed a 7 % weight loss. This weight loss was due to the removal of absorbed water molecules. The second step, which was observed between 100 °C and 350 °C, showed a 4 % weight loss. This weight loss was due to the burning of the nitrate salts and fuels present in the precursors [12]. The final step, which was observed at around 475 °C, showed a weight loss of 9 %. This was when the active reaction took place, and the precursors tended to form the compound. However, the formation of the compound was completed at around 750 °C with an unavoidable further heat loss of 1 - 2 %. Hence, a total of approximately 21 - 22 % heat loss was inevitable in the process of synthesizing the final product during the combustion process. This type of thermal behavior has been observed invariably with respect to the precursors employed in the present study towards the synthesis of the $LiNi_{0.4}Mn_{0.4}Co_{0.2}O_2$ compound [13]. Thus, it may be concluded from the observed TGA pattern that the formation temperature of a $LiNi_{0.4}Mn_{0.4}Co_{0.2}O_2$ compound could be as low as 600 °C; however, a higher degree of crystallinity would require a temperature as high as 750 °C for the final product. The effect of heating time in enhancing the degree of crystallinity is further substantiated from X-ray diffraction (XRD) analysis results.

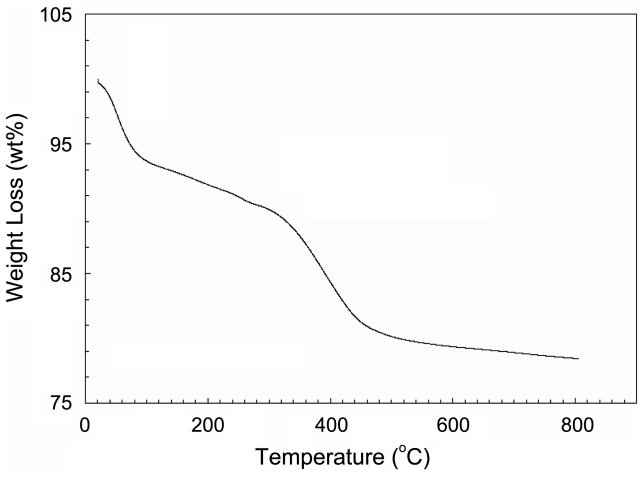

Fig. 1. Thermo gravimetric analysis curve of $LiNi_{0.4}Mn_{0.4}Co_{0.2}O_2$ precursor.

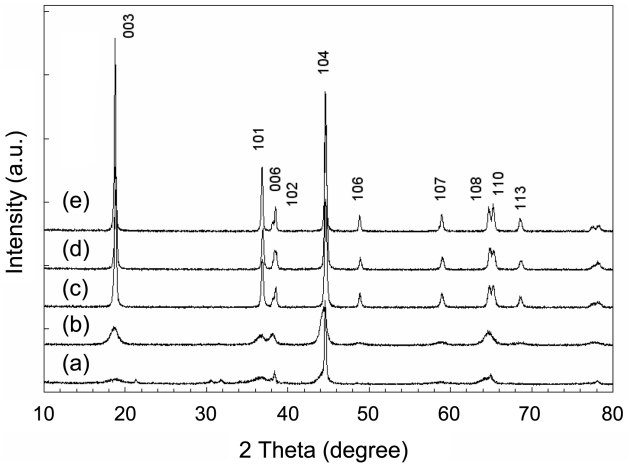

Fig. 2. X-ray diffraction patterns of $LiNi_{0.4}Mn_{0.4}Co_{0.2}O_2$ obtained at (a) 300 °C, (b) 600 °C, (c) 750 °C (3hrs), (d) 750 (12 hrs), and (e) 750 °C (24 hrs).

X-ray diffraction analysis was carried out on the synthesized product at various preparation stages of the $LiNi_{0.4}Mn_{0.4}Co_{0.2}O_2$ compound to monitor the phase purity and structure. Figure 2 shows the X-ray diffraction patterns for samples heated at 300 °C and 600 °C for 3 hrs and at 750 °C for 3, 12, and 24 hrs, respectively. The XRD patterns in Fig. 2 show that the powders are iso-structural with α-$NaFeO_2$, space group R3m, in which the transition metal atoms Ni, Mn, and Co are randomly distributed on the 3b sites, Li atoms are on the 3a sites, and O atoms are on 6c sites, respectively. It can be seen from Fig. 2 that a completely amorphous structure is obtained for the precursor powder heated at 300 °C. The XRD pattern for the sample heated at 600 °C showed that peaks was not clear and a crystallization process was not sufficient at this temperature. The same materials heated at 750 °C for 3 hrs are well crystallized into phase-pure $LiNi_{0.4}Mn_{0.4}Co_{0.2}O_2$ powders without any development of minor impurity phases. Therefore, it is understood that a minimum temperature of 750 °C is required for the formation of a single-phase product. For the sample heated at 750 °C for 3 hrs, the XRD pattern was well defined and showed hexagonal doublets (006)/(102) and (108)/(110) with a clear splitting, which indicated that the samples had a high degree of crystallinity, good hexagonal ordering, and typical layered characteristics [14]. Based on the above results, it can be concluded that the minimum temperature required for complete hexagonal ordering is 750 °C.

After the optimal heating temperature was identified as 750 °C, the influence of heating times of 3, 12, and 24 hrs was studied. As the heating time increased, the diffraction peaks became sharper and higher due to an increase in the crystallinity of the product. The variation of lattice parameters, such as a, c, c/a, R-factor, I(003)/I(104), and unit cell volume of the $LiNi_{0.4}Mn_{0.4}Co_{0.2}O_2$ samples with respect to heating times are summarized in Table 1. A relatively large increase in the I(003)/I(104) ratio is observed for the sample heated at 750 °C for 24 hrs. When the heating time was increased from 3 to 24 hrs, the intensity ratio (003/104) increased from 0.750 to 1.347, and the intensities of (003) reflections were higher than those of corresponding (104) reflections, which indicate that these samples had good cation ordering [15, 16]. According to Reimers *et al.*[17], the R-factor, defined as the ratio of the intensities of the hexagonal characteristics doublet peaks (006) and (102) to the (101) peak, is an indicator of hexagonal ordering. By this definition, lower R-factor values means good hexagonal ordering. It was not possible to calculate the intensities of the sample heated at 600 °C. However, it can be seen that, as the heating time was increased for a constant temperature of 750 °C, i.e., 3, 12, and 24 hrs, the R-factor values decreased from 0.75 to 0.60. The low values for the R-factor showed that the sample heated at 750 °C for 24 hrs possessed good hexagonal ordering, and hence, it had better cycling performance. Furthermore, the unit cell volume observed for the $LiNi_{0.4}Mn_{0.4}Co_{0.2}O_2$ sample heated at 750 °C for 24 hrs is smaller than the unit cell volumes of the samples heated at 750 °C for 3 and 12 hrs.

Dahn *et al.*[18] reported that a material with more layered characteristics would have a lower cell volume. Hence, the lithium intercalation/deintercalation properties mainly depend on the ordering of the 3a lithium occupancy sites and the 3b transition metal ion sites. The XRD pattern of $LiNi_{0.4}Mn_{0.4}Co_{0.2}O_2$ exhibits notable similarities to that of $LiNi_{0.8}Co_{0.2}O_2$ [19], as shown in Fig. 3. The lattice parameters of the $LiNi_{0.8}Co_{0.2}O_2$ sample heated at 750 °C for 24 hrs has the largest lattice constant and unit cell volume, i.e., a = 2.862 Å, c = 14.210 Å and 100.77 Å. In addition, $LiCoO_2$ has the smallest lattice constant and unit cell volume, i.e., a = 2.8275 Å, c = 14.0825 Å and 97.47 Å. And the unit cell volume of $LiNi_{0.4}Mn_{0.4}Co_{0.2}O_2$ is 99.97 Å, which is observed in between $LiCoO_2$ and $LiNi_{0.8}Co_{0.2}O_2$. Similar results have been observed by a solid-

Table 1. Lattice parameters of the $LiNi_{0.4}Mn_{0.4}Co_{0.2}O_2$ powders

Temperature / time	a(Å)	c(Å)	c/a ratio	I_{003}/I_{104}	R-factor $[I_{006}+I_{102}/I_{101}]$	Unit cell volume (Å)
600 (3h)	2.879	14.231	4.943	0.750	-	102.031
750 (3h)	2.870	14.148	4.946	1.085	0.75	100.803
750 (12h)	2.854	14.176	4.869	1.342	0.71	100.658
750 (24h)	2.877	14.059	4.967	1.347	0.60	099.879

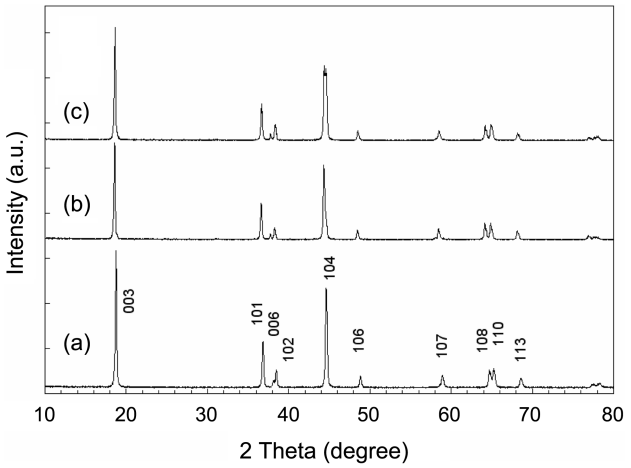

Fig. 3. X-ray diffraction patterns of (a) $LiNi_{0.4}Mn_{0.4}Co_{0.2}O_2$, (b) $LiNi_{0.8}Co_{0.2}O_2$, and (c) $LiCoO_2$.

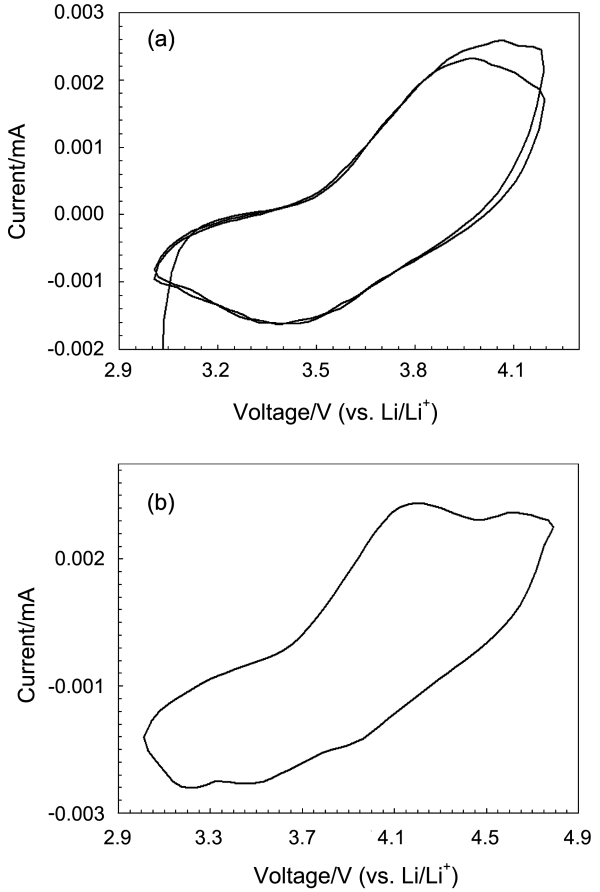

Fig. 4. Cyclic voltammograms of $Li/LiNi_{0.4}Mn_{0.4}Co_{0.2}O_2$ between 3.0 ~ 4.2 V (a) and 3.0 ~ 4.8 V (b) at a scan rate of 0.2 and 0.1 V/s at room temperature.

state method[20].

Figures 4(a) and 4(b) show the cyclic voltammogram of $LiNi_{0.4}Mn_{0.4}Co_{0.2}O_2$ synthesized at 750 °C for 24 hrs in 1M $LiPF_6$ in EC/DEC (1:1). The electrochemical performance was studied using cyclic voltammetry in the potential range from 3.0 to 4.2 V and 4.8 V vs. Li/Li^+, with Li metal as the reference and counter electrodes. The scan rates were 200 $mVsec^{-1}$ and 100 $mVsec^{-1}$, respectively. Figure 4(a) shows that an anodic peak of Li^+ deintercalation appeared at 4.0 V in a broad potential range, and an relatively lots of lithium was extracted at the cathodic peak in a broad potential range of about 3.4 V. Cyclic curves on the first cycle differed from those on the second cycles with respect to a voltage range from 3.0 to 4.2 V, in which oxidation-reduction reactions occurred. This was due to the large irreversible loss of capacity at the first cycle[21]. Moreover, the large deintercalation currents seen in the cyclic voltammogram agreed with the first cycling capacities[22]. The cyclic voltammogram of the $LiNi_{0.4}Mn_{0.4}Co_{0.2}O_2$ systems (Fig. 4(b)) showed an oxidation broad peak potential at 4.1V with a prominent shoulder at 4.0 V corresponding to the redox of Co^{3+} to Co^{4+} [23, 24]. In addition, the oxidation and reduction broad peak at 4.6 and 3.6 V was attributable to the redox of Ni^{2+} to Ni^{4+} and the reduction potential of Mn^{4+} to Mn^{3+} at 3.2 V vs. Li. These peaks illustrate well the reversibility of this material upon the deintercalation and intercalation of lithium ions over the potential range 3.0 ~ 4.8 V versus the Li/Li^+ reference electrode. These results are in agreement with those of Lu *et al.*[25], although they used $Li_{2/3}[Co_xNi_{1/3-x/2}Mn_{2/3-x/2}]O_2$ with x=0, 1/12, 1/8, 1/6, and 1/4 measured between voltages of 2.5 and 4.2 V. The voltammograms in Fig. 4 (a) and (b) suggest that the $LiNi_{0.4}Mn_{0.4}Co_{0.2}O_2$ prepared in the present study exhibits electrochemical activity.

Generally, electrochemical impedance studies have led to a better understanding of many aspects of lithium cells, including insight into failure mechanisms [26], self-discharges [27] lithium-cycling efficiencies [28], interfacial phenomena between electrodes and electrolytes [29], and lithium cation diffusions in electrodes and electrolytes [30]. Even so, cathodes have received relatively little attention, perhaps because problems related to lithium anodes are the main concern for commercialization of rechargeable lithium batteries. However, with advancements in lithium and lithium-ion battery technology, attention is shifting gradually to cathodes and their related problems. One of the major factors affecting the capacity fade and voltage drop during discharge in the lithium battery is the impedance rise in the materials during continuous cycling [31]. Electrochemical impedance measurements were recorded for both as-assembled and fully-charged states. Figure 5 showed a comparison of the Nyquist plot for the $Li/LiNi_{0.4}Mn_{0.4}Co_{0.2}O_2$ before and after the first cycle. The Nyquist plots were measured at the same potential of 3.2 V and the same electrode after 1st cycle. The high-frequency semicircle in the spectrum of the fresh electrode is much higher than that of the cycled electrode[32]. Figure 6 shows the impedance spectra of $Li/LiNi_{0.4}Mn_{0.4}Co_{0.2}O_2$ cells at

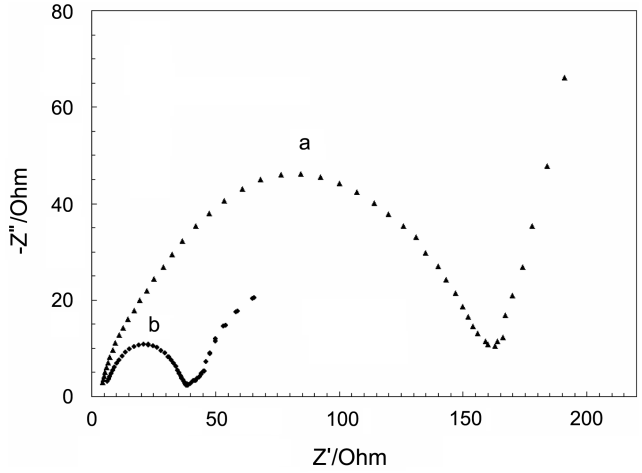

Fig. 5. Comparison between the Nyquist plots of as assembled and after the 1st cycle completed $Li/LiNi_{0.4}Mn_{0.4}Co_{0.2}O_2$ cell at 3.2V. (a) as-assembled cell and (b) after the 1st cycle.

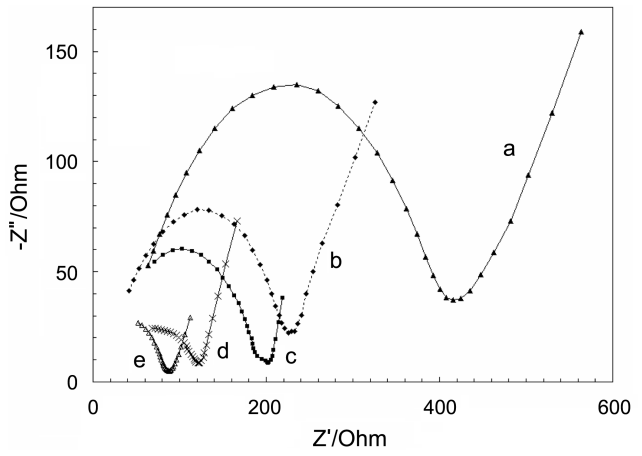

Fig. 6. Nyquist plots of the $Li/LiNi_{0.4}Mn_{0.4}Co_{0.2}O_2$ cell recorded at different state of charge such as (a) 0 % , (b) 25 %, (c) 50 %, (d) 75 %, and (e) 100 % SOC.

state-of-charge (SOC) values of 0 %, 25 %, 50 %, 75 %, and 100 %. A semicircle in the high-frequency region and a spike in the low-frequency region characterized each impedance spectrum. The semicircle was attributed to the presence of a passivation film on the oxide surface [33, 34]. The low-frequency spike was the arc of an incomplete semicircle, which was attributed to the charge-transfer resistance of the electrochemical reaction. It can be seen from Fig. 6 that the charge transfer resistance decreased with increasing a charge voltage, which indicates that the $LiNi_{0.4}Mn_{0.4}Co_{0.2}O_2$ materials became more conductive at a highly charged state. In a fully charged state (SOC 100 %), the $LiNi_{0.4}Mn_{0.4}Co_{0.2}O_2$ material showed the lowest Rct values (85 Ohms). At high charging voltages, the $LiNi_{0.4}Mn_{0.4}Co_{0.2}O_2$ materials turned into good conductors, and it could impact on the high drain capability of the systems [35]. And the delithiation processes were accompanied by changes in the volume of the cathode and thickness of its surface layer[36].

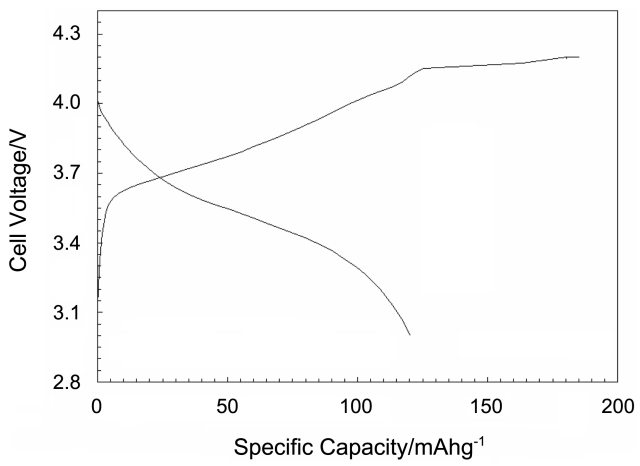

Fig. 7. Charge-discharge profile of $Li/LiNi_{0.4}Mn_{0.4}Co_{0.2}O_2$ cell cycled between 3.0 and 4.2 V at a current density of 0.2 $mAcm^{-2}$.

Figure 7 showed the charge-discharge behaviors of $LiNi_{0.4}Mn_{0.4}Co_{0.2}O_2$ materials heated at 750 °C for 3 hrs. The samples were charged/dicharged galvanostatically at a 0.1C rate between 3.0 and 4.2 V. A $Li/LiNi_{0.4}Mn_{0.4}Co_{0.2}O_2$ cell initially delivers the charge and discharge capacities of 185.1 and 120.3 $mAhg^{-1}$ at a current density of 0.2 $mAcm^{-2}$. The large first cycle irreversibility of the same materials is reflected in the cyclic voltammograms (Fig. 7). Lee *et al.* have presented a Rietveld refinement analysis of the neutron diffraction data for a $LiNi_{0.8}Co_{0.2}O_2$ compound. Their analysis makes clear that extra nickel ions occupying the lithium 3a site are the main cause for the capacity loss in the first cycling. The ionic radius of Ni^{2+} is 0.69 Å and is close to that of Li^{+} (0.76 Å). Therefore, a small amount of Ni may occupy the 3a Li sites. If this occurs, the same amount of displaced Li atoms will

Table 2. Electrochemical properties of $Li/LiNi_{0.4}Mn_{0.4}Co_{0.2}O_2$ cells with a cutoff voltage of 4.2 V for sample heated at different hours

Heating time (hrs)	1st cycle ($mAhg^{-1}$)			20th cycle ($mAhg^{-1}$)		
	Charge capacity	Discharge capacity	Irreversible capacity	Charge capacity	Discharge capacity	Irreversible capacity
3	185.1	120.3	64.8	93.6	89.9	3.7
12	185.3	134.1	51.3	115.4	112.8	2.6
24	196.4	141.7	54.7	131.9	128.9	3.0

Table 3. Electrochemical properties of $Li/LiNi_{0.4}Mn_{0.4}Co_{0.2}O_2$ cells with a cutoff voltage of 4.4 V for sample heated at different hours

Heating time (hrs)	1st cycle ($mAhg^{-1}$)			20th cycle ($mAhg^{-1}$)		
	Charge capacity	Discharge capacity	Irreversible capacity	Charge capacity	Discharge capacity	Irreversible capacity
3	180.8	132.7	48.1	124.6	123.1	1.5
12	185.8	148.5	37.2	140.4	136.1	4.3
24	186.3	166.3	20.1	156.6	147.1	9.4

Table 4. Electrochemical properties of $Li/LiNi_{0.4}Mn_{0.4}Co_{0.2}O_2$ cells with a cutoff voltage of 4.6 V for sample heated at different hours

Heating time (hrs)	1st cycle CC ($mAhg^{-1}$)			20th cycle ($mAhg^{-1}$)		
	Charge capacity	Discharge capacity	Irreversible capacity	Charge capacity	Discharge capacity	Irreversible capacity
3	183.9	141.6	42.3	137.2	130.2	7.0
12	187.5	165.0	22.5	160.8	154.1	6.6
24	195.4	181.4	14.0	165.5	159.5	6.0

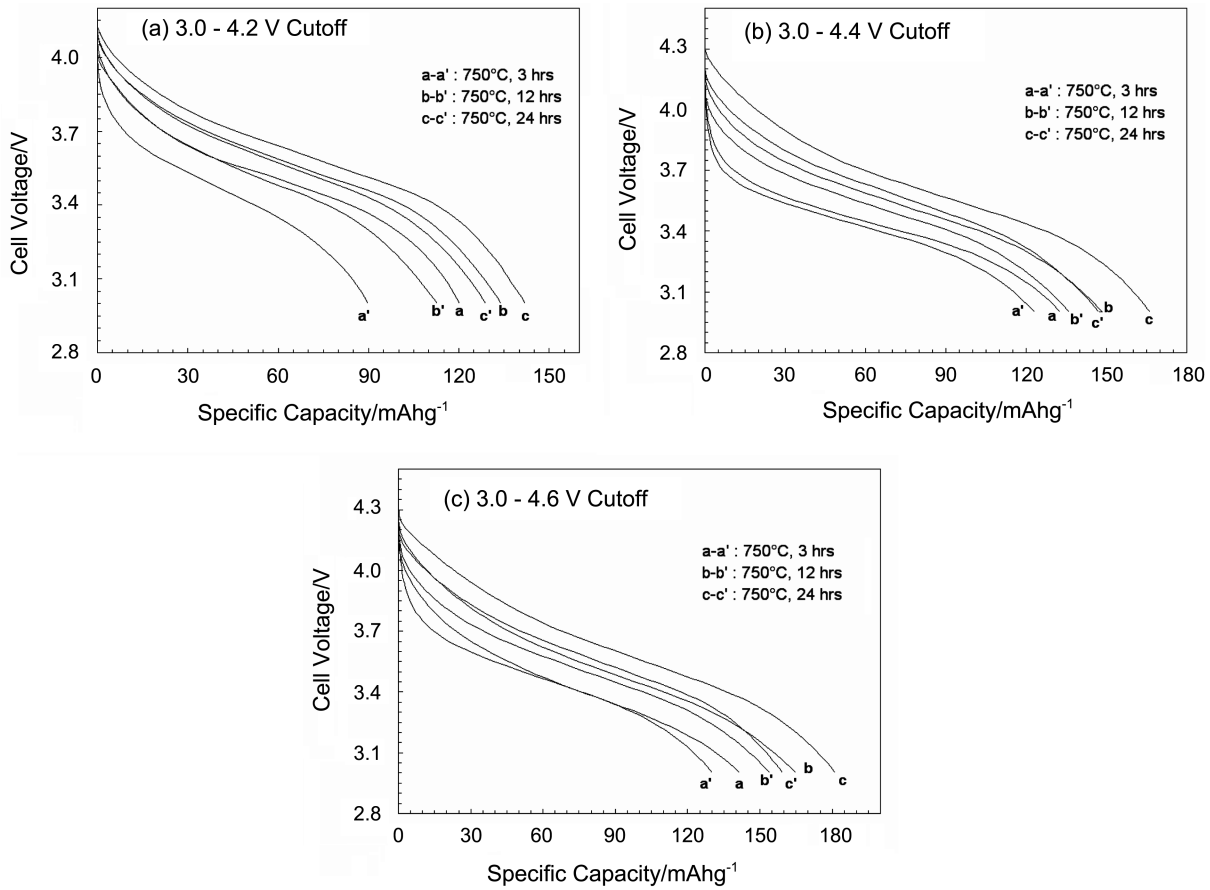

Fig. 8. Specific discharge capacity obtained the1st and 20th cycles with cutoff voltage for $Li/LiNi_{0.4}Mn_{0.4}Co_{0.2}O_2$ cells.

occupy the 3b Ni site. In addition, once a certain irreversible capacity is obtained in the first cycle, further intercalation / deintercalation of lithium ions occurs only at the lithium site excluding the vacant sites around the extra nickel ions. Hence, a good reversibility is maintained after the first cycling [38]. The effects of charging cutoff voltages were studied for the samples heated at 750 °C for 3, 12, and 24 hrs. Variations in the discharge capacity with respect to cut-off voltage and heating time for the compound $LiNi_{0.4}Mn_{0.4}Co_{0.2}O_2$ are shown in Fig. 8 (a), (b) and (c).

Electrochemical properties of the $LiNi_{0.4}Mn_{0.4}Co_{0.2}O_2$ samples prepared at 750 °C with different charging cutoff voltages were given in Tables 2, 3, and 4, respectively. After the sample prepared at 750 °C for 12 hrs was cycled for 20 cycles at cutoff voltages of 4.2, 4.4, and 4.6 V, the sample exhibited specific discharge capacities of 112.8, 136.1, and 154.1 $mAhg^{-1}$ and irreversible capacities of 2.6, 4.3, and 6.6 $mAhg^{-1}$, respectively. However, the decrease in the specific discharge capacities for samples prepared at 750 °C for 3 hrs and 12 hrs, with respect to charge cutoff voltages of 4.2, 4.4, and 4.6 V, is mainly attributed to a lack of hexagonal ordering, i.e., a lack of ordering in lithium ion and transition metal ions sites and lower crystallinity [37]. Generally, due to the formation of this oxide, high temperature and long heating times are required to form a well-ordered $LiNi_{0.4}Mn_{0.4}Co_{0.2}O_2$ phase. Therefore, samples prepared at 750 °C for 3 and 12 hrs showed lower discharge capacities than those of the samples heated longer (24 hrs) at the same temperature. It can be seen from Tables 2, 3, and 4 that good capacity retention was obtained after 20 cycles for all samples prepared at 750 °C for 24 hrs: the discharge capacities of the samples were 128.9, 147.2, and 159.5 $mAhg^{-1}$ with cutoff voltages of 4.2, 4.4, and 4.6 V, respectively. These results are in agreement with those of MacNeil *et al.*[39]; however, $LiNi_xCo_{1-2x}Mn_xO_2$ (x=0.0125 to 0.45) showed a discharge capacity of 120 $mAhg^{-1}$ at a cutoff voltage of 4.2 V compared to a discharge capacity of 145 $mAhg^{-1}$ at a higher cutoff voltage of 4.4 V, and the study also reported that most of the discharge capacity was attained below 3.8 V, as the nickel content was increased.

4. CONCLUSIONS

Single-phase electro-active $LiNi_{0.4}Mn_{0.4}Co_{0.2}O_2$ compounds were prepared via the combustion process, using glycine as a fuel agent at low temperature. Cyclic voltammetry studies showed that large and broad peaks around 4.1 V were related to the redox couple Co^{3+} to Co^{4+}, while small broad peaks around 4.6 V corresponded to the redox couple Ni^{2+} to Ni^{4+}. Electrochemical impedance studies performed at different states of charging voltages showed a decrease in the charge transfer resistance as the lithium was removed from the $LiNi_{0.4}Mn_{0.4}Co_{0.2}O_2$ materials. The charge-discharge behaviors of the systems were studied between 3.0 and 4.2 V and between 4.4 and 4.6 V at room temperature. The $LiNi_{0.4}Mn_{0.4}Co_{0.2}O_2$ prepared at 750 °C for 24 hrs delivered discharge capacities of 181.4 and 159.5 $mAhg^{-1}$ after the 1st and 20th cycles in the voltage region between 3.0 and 4.6 V.

ACKNOWLEDGMENT

This research was supported by a grant (code no. 05K1501-01910) from the Center for Nanostructured Materials Technology to support the 21st Century Frontier R&D Programs of the Ministry of Science and Technology, Korea.

REFERENCES

1. R. Koksbang, J. Barker, H. Shi, and M. Y. Saidi, *Solid State Ionics* **84**, 1 (1996).
2. T. Ohzuku, A. Ueda, and M. Nagayama. *J. Electrochem. Soc.* **140**, 1862 (1993).
3. J. R. Dahn, U. Von Sacken, and C. A. Michal, *Solid State Ionics* **44**, 87 (1990).
4. A. Rougier, P. Gravereau, and C. Delmas, *J. Electrochem. Soc.* **143**, 1168 (1996).
5. Y. K. Sun, D. W. Kim, and Y. M. Choi, *J. Power Sources* **79**, 231 (1999).
6. A. Kinoshita, K. Yanagida, A. Yanai, Y. Kida, A. Funahashi, T. Nohrna, and I. Yonezu, *J. Power Sources* **102**, 283 (2001).
7. K. M. Kim, J. C. Kim, N. G. Park, K. S. Ryu, and S. H. Chang, *J. Power Sources* **123**, 69 (2003).
8. Y. Makimura and T. Ohzuku, *J. Power Sources* **119-121**, 156 (2003).
9. Z. Lu and J. R. Dahn, *J. Electrochem. Soc.* **149**, 744 (2002).
10. Z. Lu, R. A. Donaberger, C. L. Thomas, and J. R. Dahn, *J. Electrochem. Soc.* **149**, 1083 (2002).
11. Z. Lu, D. D. MacNeil, and J. R. Dahn, *J. Phys. Chem.* A **105**, 4430 (2001).
12. G. T. K. Fey, R. F. Shiu, V. Subramanian, J. G. Chen, and C. L. Chen, *J. Power Sources* **103**, 265 (2002).
13. N. Kalaiselvi, P. Kalyani, and N. Muniyandi, *Mater. Chem. and Phys.* **77**, 662 (2002).
14. G. T. K. Fey, Z. F. Wang, and T. P. Kumar, *Ionics* **8**, 351 (2002).
15. Y. Gao, M. V. Yakovieva, and W. B. Ebner, *Electrochem. Solid-State Lett.* **1**, 117 (1998).
16. J. Kim, P. Fulmer, and A. Manthiram, *Mater. Res. Bull.* **34**, 571 (1999).
17. J. R. Reimers, E. Rossen, C. D. Jones, and J. R. Dahn, *Solid State Ionics* **61**, 335, (1993).
18. J. R. Dahn, U. Von Sacken, and C. A. Michal, *Solid State Ionics* **44**, 87 (1990).
19. P. Periasamy, H. Kim, S. Na, S. Moon, and J. Lee, *J. Power Sources* **132**, 213 (2004).
20. N. Yabuuchi and T. Ohzuku, *J. Power Sources* **119-121**, 171 (2003).
21. S. Madhavi, G. V. Subba Rao, B. V. R. Chowdari, and S. F. Y. Li, *J. Power Sources* **93**, 156 (2001).
22. G. T. K. Fey, J. G. Chen, V. Subramanian, and T. Osaka, *J. Power Sources* **112**, 384 (2002).
23. A. Manthiram and J. Kim, *Chem. Mater.* **10**, 2895 (1998).
24. T. Ohzuku, A. Ueda, M. Nagayama, Y. Iwakoshi, and H. Komori, *Electrochim. Acta* **38**, 1159 (2003).
25. Z. Lu, R. A. Donaberger, C. L. Thomas, and J. R. Dahn, *J. Electrochem. Soc.* **149**, 1083A (2002).

26. R. Koksbang, I. I. Olsen, P. E. Tonder, N. Knudsen, and D. Fauteux, *J. Appl. Electrochem.* **21**, 301 (1991).
27. G. Pistoia, A. Antonin, R. Rosati, and D. Zane, *Electrochim. Acta* **41**, 2683 (1996).
28. G. Montesperelli, P. Nunziante, M. Pasquali, and G. Pistoia, *Solid State Ionics* **37**, 149 (1990).
29. M. Gaberscek and S. Pejovnik, *Electrochim. Acta* **41**, 1137 (1996).
30. F. Capuano, F. Croce, and B. Scrosati, *J. Electrochem. Soc.* **138**, 1918 (1991).
31. R. P. Ramasamy, P. Ramadass, B. S. Haran, and B. N. Popov, *J. Power Sources* **124**, 155 (2003).
32. M. D. Levi, K. Gamolsky, D. Aurbach, U. Heider, and R. Oesten, *Electrochim. Acta* **45**, 1781 (2000).
33. S. Rodrigues, N. Munichandraiah, and A. K. Shukla. *J. Solid State Electrochem.* **3**, 397 (1999).
34. P. Suresh, A. K. Shukla, and N. Munichandraiah, *J. Power Sources* **112**, 665 (2002).
35. G. T. K. Fey, C. Z. Lu, and T. Prem Kumar, *J. Power Sources* **115**, 332 (2003).
36. M. D. Levi, K. Gamolsky, D. Aurbach, U. Heider, and R. Oesten, *Electrochim. Acta* **45**, 1781 (2000).
37. K. Lee and K. Kim, in Lithium Batteries (eds. S. Surampudi, R. A. Marsh, A. Ogumi, and J. Prakash), p. 257, *The Electrochemical Society Proceedings Series,* Pennington, NJ (2000).
38. R. D. Shannon, *Acta Crystallography A: Crystal Physics and Diffraction Theory,* p. 751, New York (1976).
39. D. D. MacNeil, Z. Lu, and J. R. Dahn, *J. Electrochem. Soc.* **149**, 1332A (2002).